

PORE AND MICROCRYSTAL STRUCTURE OF CO-PYROLYSIS CHAR FROM POLYVINYL CHLORIDE AND BITUMINOUS COAL

Haiyu Meng¹, Shuzhong Wang^{2,*}, Zhiqiang Wu³, Jun Zhao², Lin Chen², Jiake Li¹

1 State Key Laboratory of Eco-hydraulics in Northwest Arid Region, Institute of Water Resources and Hydro-electric Engineering, Xi'an University of Technology, Xi'an, Shaanxi, 710048, P.R. China

2 Key Laboratory of Thermo-Fluid Science and Engineering, Ministry of Education, School of Energy and Power Engineering, Xi'an Jiaotong University, Xi'an, Shaanxi, 710049, P.R. China

3 School of Chemical Engineering and Technology, Xi'an Jiaotong University, Xi'an, Shaanxi, 710049, P.R. China

ABSTRACT

The physico-chemical structure of co-pyrolysis char significantly affects its gasification reactivity. Pore distribution and microcrystal structure of co-pyrolysis char from polyvinyl chloride (PVC) and bituminous coal were investigated by specific surface area analyzer and X-ray diffraction. Based on fractal theory and deconvolution method, the influence of PVC on co-pyrolysis char structure was analyzed quantitatively. The results showed that the specific surface area of co-pyrolysis char increased slightly compared with PVC char. Similar to the PVC char, the pore size distribution of co-pyrolysis char was wide and uniform. The ordering of carbon microcrystal structure of co-pyrolysis char was promoted by the addition of PVC. This study can provide basic data for exploring the relationship between gasification characteristics and structure parameters of co-pyrolysis char.

Keywords: co-pyrolysis char, pore distribution, microcrystal structure, polyvinyl chloride, bituminous coal

1. INTRODUCTION

Co-pyrolysis is the critical initial stage of co-gasification of plastics and coal. The product properties of co-pyrolysis process especially the physico-chemical structure of co-pyrolysis chars have important effect on the subsequent reaction process [1-4]. The addition of plastic would influence the spatial structure and surface morphology of co-pyrolysis chars [5, 6]. It is very important to investigate the impact of plastic on the

structure evolution of co-pyrolysis char for their efficient utilization of plastics and coal.

The pores are the diffusion channels of gasification medium and some products during char gasification process, while the active sites on char surface are the major places of chemical reactions [1, 7]. Thus, the pore structure and surface both have important effects on the reactivity of chars. Havelcova et al. [6] found that as the waste plastics (PET) mass ratio increased, the mesopores in co-pyrolysis chars increased, but the micropores decreased. The char reactivity is also affected by the microcrystal structure. The evolution of microcrystal structure of co-pyrolysis chars from plastic and coal has been reported by some investigators [5, 6]. The addition of PET increased the ordered degree of carbon microcrystal structure of co-pyrolysis chars when the plastic mass ratio was relatively low, while the improvement of ordered degree was inhibited as the plastic blending ratio increased to 20% [6]. However, few efforts have been devoted to exploring the impact of polyvinyl chloride (PVC) on pore and microcrystal structure evolution of co-pyrolysis chars.

This paper aims to investigate the effects of PVC on the structure evolution of co-pyrolysis char. Physico-chemical structure characteristics, including specific surface area, pore structure and microcrystal structure were explored. Fractal theory was applied to quantitatively evaluate the complexity of pore space. Furthermore, the influence of PVC on the carbon microcrystal structure of co-pyrolysis chars was revealed by peak fitting of XRD spectrum.

2. EXPERIMENTAL

2.1 Materials

The PVC powder was purchased from Aladdin Industrial Corporation (CAS number: 9002-86-2). The bituminous coal (SM) was collected from Shaanxi province. The particles of less than 74 μm were chosen for the experiments. The blended samples of PVC and SM were named as "PVCSM3-7", "PVCSM1-1", and "PVCSM7-3", which represented that the mass ratios of PVC in the mixtures were respectively 30%, 50%, and 70%. Table 1 presents the composition analysis results of the PVC and SM. The volatile matter content of PVC was much higher than that of SM.

Table 1. Proximate and ultimate analysis of the samples

Material	PVC	SM
Proximate analysis (wt %, ad)		
Moisture	0	10.15
Ash	0	5.95
Volatile matter	92.14	31.06
Fixed carbon	7.86	52.84
Ultimate analysis (wt %, daf)		
Carbon	39.66	78.89
Hydrogen	5.24	3.09
Nitrogen	-	1.07
Sulfur	0.06	0.86
Oxygen (by difference)	-	16.09
Chlorine	55.04	-

2.2 Apparatus and methods

2.2.1 Char preparation

The char samples of PVC, SM and their blends were prepared applying a laboratory-scale tube reactor (inside diameter of 35 mm, length of 800 mm), which was heated by an electrical resistance furnace. The heating area of the furnace is 600 mm of length, 40 mm of inner diameter, 1200 $^{\circ}\text{C}$ of maximum heating temperature, and 2 kW of heating power. The high purity nitrogen (99.999%) was used as sweep gas with flow rate of 100 $\text{mL}\cdot\text{min}^{-1}$ controlled by a mass flow meter. The reactor was firstly heated from ambient temperature to 900 $^{\circ}\text{C}$, and kept constant for 10 min. Then the samples were fed into the constant temperature zone and the rapid

pyrolysis experiments started. The temperature of the furnace was kept at 900 $^{\circ}\text{C}$ for 15 min after the samples were fed into the reactor. The char samples were collected in sample bags for further analysis after cooling to room temperature. The char samples are abbreviated as follows: PVC char, SM char, and PVCSM char.

2.2.2 Fractal analysis on char sample

Fractal theory can be applied to describe the irregular complex specific surface area and pore structure of solids, and the fractal dimension has been widely used as a quantitative indicator [8-10]. It has been found that the pore structures of coal char have characteristics of statistic self-similarity and scale invariance. Thus, the fractal dimension can be applied to quantitatively describe complex and irregular pore structure in char samples [11-14]. At present, there is few investigations on whether the fractal dimension can describe the pore structure characteristics of co-pyrolysis char from plastics and coal. Avnir and Jaronice [8] advanced the following method to compute the fractal dimension:

$$\ln \left[\frac{V}{V_0} \right] = C + (D - 3) \left[\ln \left(\frac{P_0}{P} \right) \right] \quad (1)$$

where V is the N_2 adsorption capacity under relative pressure P/P_0 ($\text{mL}\cdot\text{g}^{-1}$), P_0 is the saturated vapor pressure of gas adsorption (Pa), V_0 is the saturated adsorption capacity of single molecular ($\text{mL}\cdot\text{g}^{-1}$), C is a constant, and D is the fractal dimension. The fractal dimension of char samples reflects the stereoscopic degree of pore surface structure, and the value is between 2 and 3. The value of 2 indicates that the pore structure is regular and the pore surface is smooth, the value of 3 demonstrates that the pore structure is irregular and the pore surface is rough.

2.2.3 Carbon microcrystal structure analysis

The carbon microcrystal structures existing in pyrolytic chars from carbon-based solid materials are formed by the superposition of multi-layers of aromatic layers. The length and width of the aromatic layers are called the crystallite size (L_a), and the distance between the aromatic layers is represented by the crystal plane spacing (d_{002}). The average stacking thickness of each microcrystalline layer, which is also called the average stacking height, is labeled as L_c . The diffraction peak (002) located between 20-30 $^{\circ}$ reflects the degree of parallel and azimuthal orientation of the aromatic layers in the microcrystal structure. The diffraction peak (100) located between 40-50 $^{\circ}$ characterizes the size of aromatic layer. The microcrystal structure parameters

are calculated via Bragg and Scherrer equations [15, 16]. The formula are as follows:

$$d_{002} = \frac{\lambda}{2 \sin \theta_{002}} \quad (2)$$

$$L_c = \frac{K_1 \lambda}{\beta_{002} \cos \theta_{002}} \quad (3)$$

$$L_a = \frac{K_2 \lambda}{\beta_{100} \cos \theta_{100}} \quad (4)$$

where d_{002} is the crystal plane spacing (nm), L_c is the average stacking thickness (nm), L_a is the average crystallite size (nm), λ is the wavelength of X-ray (Å), θ is the diffraction angle (degree), β is the half-peak width of diffraction peak(rad), and K is the correction factor (CuK α , $\lambda=1.54178\text{\AA}$, $K_1=0.94$, $K_2=1.84$).

Some investigators analyzed the XRD spectrums of pyrolytic chars applying the “peak-fitting” method. It was found that there usually existed three different forms of carbon structure in char samples: the carbon structure with poor quality (broad amorphous carbon), carbon structure with a better setting degree (relatively broad turbostratic carbon) and graphite-like carbon structure (graphitic carbon) [17-19]. The carbon structure above can be identified by decomposing the crystal plane diffraction peak (002) through peak fit. The carbon-containing substances can be divided into two structural forms, including the relatively poorly-defined microcrystal structures (P) and microcrystal structures with relatively good shape setting (G) [17]. Further quantitative calculations of the two microcrystal structures are as follows:

$$d_{002,P} = \frac{\lambda}{2 \sin(\theta_{002,P})} \quad (5)$$

$$d_{002,G} = \frac{\lambda}{2 \sin(\theta_{002,G})} \quad (6)$$

$$L_{c,P} = \frac{K_1 \lambda}{\beta_{002,P} \cos(\theta_{002,P})} \quad (7)$$

$$L_{c,G} = \frac{K_1 \lambda}{\beta_{002,G} \cos(\theta_{002,G})} \quad (8)$$

where $d_{002,P}$ and $d_{002,G}$ is the crystal plane spacing of the P and G (nm), $L_{c,P}$ and $L_{c,G}$ is the average stacking thickness of the P and G (nm), λ is the wavelength of X-ray (Å), $\theta_{002,P}$ and $\theta_{002,G}$ is the diffraction angle of the P and G ($^\circ$), $\beta_{002,P}$ and $\beta_{002,G}$ is the half-peak width of the P and G peak (rad). Furthermore, the overall microcrystal structure parameters can be obtained by weighted average of the relevant parameters of the P peak and G peak:

$$d_{002,m} = x_P d_{002,P} + x_G d_{002,G} \quad (9)$$

$$L_{c,m} = x_P L_{c,P} + x_G L_{c,G} \quad (10)$$

$$x_P = \frac{S_P}{S_P + S_G} \quad (11)$$

$$x_G = \frac{S_G}{S_P + S_G} \quad (12)$$

where $d_{002,m}$ is the average crystal plane spacing of the char sample (nm), $L_{c,m}$ is the average stackin thickness (nm), x_P is the area ratio of P peak, x_G is the area ratio of G peak, S_P is the peak area of P, and S_G is the peak area of G. In this paper, the crystal plane spacing d_{002} and the average stacking thickness L_c of the char samples were calculated by Eqs. (9) and (10), and the average crystallite size L_a was computed by Eq. (4).

3. RESULTS AND DISCUSSION

3.1 Pore structure and specific surface area

The adsorption-desorption isotherms of individual and co-pyrolysis char samples are presented in Fig. 1. According to the classification of solid-gas adsorption isotherms by IUPAC [20], the adsorption isotherms of PVC char and SM char were typical type II isotherms. The isotherm of PVC char was nearly consistent in the whole pressure range, and the adsorption loop was not obvious. This phenomenon indicated that the pore structures in PVC char may be mainly composed of relatively closed capillary at one end and the impermeable holes varying widely in size. The adsorption capacity of SM char increased rapidly when the relative adsorption pressure was low. This phenomenon called micropore filling indicated that SM char had abundant micropore and mesopore with size of about 2 nm. The adsorption loop of SM char was obvious, which indicated that the pore structure of this char was complex. The pore shape was not cylindrical holes with smooth surface, but had both impermeable and open holes.

The adsorption curves of PVC/SM char samples were similar to type II isothermal adsorption line, which corresponded to the transition from single-layer adsorption to multi-layer adsorption under low pressure. With the increase of the relative pressure, the adsorption capacity gradually increased. When the relative adsorption pressure exceeded 0.8, the adsorption capacity of co-pyrolysis chars increased rapidly because of the occurrence of capillary condensation, which indicated that there existed a certain number of

mesopores and macropores in the co-pyrolysis chars. The adsorption capacity of co-pyrolysis chars had little change compared with that of PVC char.

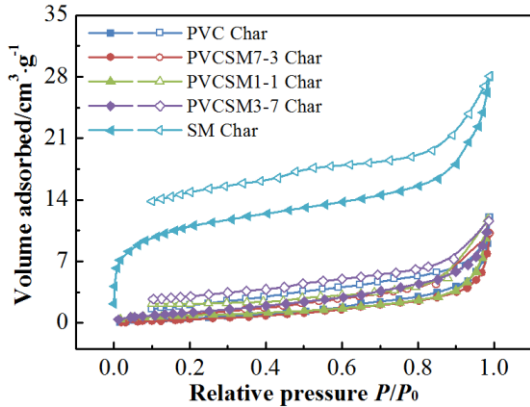


Fig. 1. The N₂ adsorption-desorption isotherms of PVCSM char samples

Figs. 2 and 3 respectively show the pore size and specific surface area distributions of PVCSM char samples. The pore size and specific surface area distributions of PVCSM char samples are basically similar with PVC char. The co-pyrolysis chars had less pore structures, and the pore size distributions were wide and uniform.

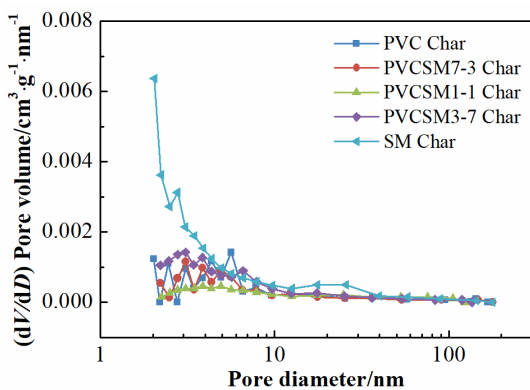


Fig. 2. Pore size distributions of PVCSM char samples

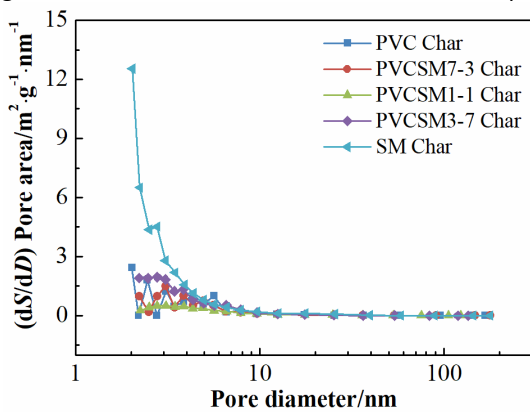


Fig. 3. The specific surface area distributions of PVCSM char samples

Table 2 shows the results of the specific surface area and pore size parameters of PVCSM char samples. It can be observed from Table 2 that the specific surface area of PVCSM char increased slightly with the increment of SM blending ratio. The average pore size of PVCSM chars decreased with increasing the SM blending ratio. The fractal dimension of the residual char samples is listed in Table 3. The fractal dimension of PVC char was smaller than that of SM char, which was due to the plastic deformation of PVC during pyrolysis, resulting in pore expansion and smooth pore surface. As the SM blending ratio increased, the fractal dimension increased indicating that the complexity of pore surface of co-pyrolysis char increased.

Table 2. Specific surface area and pore size parameters of PVCSM char samples

Samples	Surface area /m ² ·g ⁻¹	Pore volume /cm ³ ·g ⁻¹	Average pore size/nm
PVC Char	2.17	0.01862	15.10
PVCSM7-3 Char	3.07	0.01575	14.85
PVCSM1-1 Char	3.15	0.01825	11.32
PVCSM3-7 Char	4.82	0.01792	10.58
SM Char	35.95	0.04342	9.30

Table 3. Fractal dimension of PVCSM char samples

PVC mass ratio	PVCSM char	
	<i>D</i>	<i>R</i> ²
0	2.72	0.9962
0.3	2.53	0.9663
0.5	2.44	0.9982
0.7	2.40	0.9459
1	2.37	0.9444

3.2 Carbon microcrystal structure

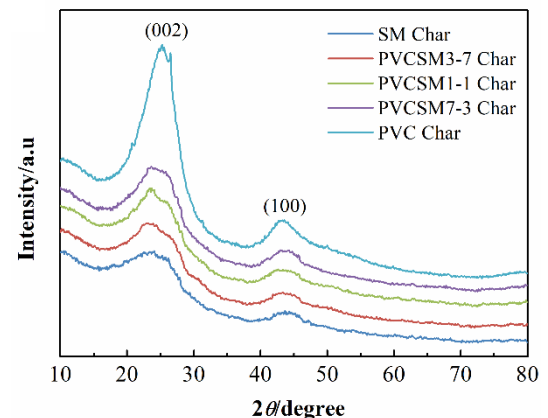


Fig. 4. The XRD spectrums of PVCSM char samples

Fig. 4. presents the XRD spectrums of PVCSM char samples. The 002 and 100 diffraction characteristic peaks were easily found in the XRD spectra. The 002 and 100

diffraction peaks increased with the increment of PVC blending ratio, which indicated that the addition of PVC promoted the ordered degree of co-pyrolysis chars.

Table 4 lists the carbon microcrystal structure parameters of PVCSM char samples. The values of $d_{002,m}$ and L_a decreased with increasing the PVC blending ratio, and $L_{c,m}$ presented an opposite variation trend. The variation trend of parameters revealed that the ordered degree of co-pyrolysis chars was increased with the addition of PVC, which was consistent with the variation of XRD spectrums. Highly ordered carbon microcrystal structure may reduce the reactivity of co-pyrolysis char samples.

Table 4. Carbon microcrystal structure parameters of PVCSM char samples

Samples	$d_{002,m}/\text{\AA}$	$L_{c,m}/\text{\AA}$	$L_a/\text{\AA}$
SM Char	3.723	14.48	40.85
PVCSM3-7 Char	3.675	11.21	45.17
PVCSM1-1 Char	3.639	11.76	44.07
PVCSM7-3 Char	3.620	12.43	43.14
PVC Char	3.615	15.69	43.04

4. CONCLUSION

The pore and carbon microcrystal structure evolution of co-pyrolysis chars from polyvinyl chloride (PVC) and a bituminous coal (SM) were investigated in this paper. The results indicated that specific surface area of PVC char was much smaller than SM char. The specific surface area of PVCSM chars increased slightly with the addition of SM, but the effects on pore size distributions were not significant. As the PVC blending ratio increased, the ordered degree of carbon microcrystal structure of co-pyrolysis chars was enhanced.

ACKNOWLEDGEMENT

This work was financially supported by the Natural Science Basic Research Plan in Shaanxi Province of China (Grant No: 2018JQ5101), the China Postdoctoral Science Foundation (Grant No: 2018M633644XB), the National Natural Science Foundation of China (Grant No. 51606149).

REFERENCE

[1] Zhao HY, Li YH, Song Q, Liu SC, Yan J, Wang XH, et al. Investigation on the physicochemical structure and gasification reactivity of nascent pyrolysis and gasification char prepared in the entrained flow reactor. *Fuel*. 2019;240:126-37.
 [2] Wu ZQ, Ma C, Jiang Z, Luo ZY. Structure evolution and gasification characteristic analysis on co-pyrolysis char from

lignocellulosic biomass and two ranks of coal: Effect of wheat straw. *Fuel*. 2019;239:180-90.

[3] Meng HY, Wang SZ, Chen L, Wu ZQ, Zhao J. Thermal behavior and the evolution of char structure during co-pyrolysis of platanus wood blends with different rank coals from northern China. *Fuel*. 2015;158:602-11.

[4] Wu ZQ, Yang WC, Chen L, Meng HY, Zhao J, Wang SZ. Morphology and microstructure of co-pyrolysis char from bituminous coal blended with lignocellulosic biomass: Effects of cellulose, hemicellulose and lignin. *Appl Therm Eng*. 2017;116:24-32.

[5] Melendi S, Barriocanal C, Alvarez R, Diez MA. Influence of low-density polyethylene addition on coking pressure. *Fuel*. 2014;119:274-84.

[6] Havelcova M, Bicakova O, Sykorova I, Weishauptova Z, Melegy A. Characterization of products from pyrolysis of coal with the addition of polyethylene terephthalate. *Fuel Process Technol*. 2016;154:123-31.

[7] Wang GW, Zhang JL, Chang WW, Li RP, Li YJ, Wang C. Structural features and gasification reactivity of biomass chars pyrolyzed in different atmospheres at high temperature. *Energy*. 2018;147:25-35.

[8] Avnir D, Jaroniec M. An isotherm equation for adsorption on fractal surfaces of heterogeneous porous materials. *Langmuir*. 1989;5:1431-3.

[9] Jaroniec M. Evaluation of the fractal dimension from a single adsorption-isotherm. *Langmuir*. 1995;11:2316-7.

[10] El Shafei GMS, Philip CA, Moussa NA. Fractal analysis of hydroxyapatite from nitrogen isotherms. *Journal of Colloid and Interface Science*. 2004;277:410-6.

[11] Hu S, Sun XX, Xiong YH, Xiang J, Li M, Li PS. Percolation research on fractal structure of coal char. *Energy Fuels*. 2002;16:1128-33.

[12] Wang XL, He R, Chen YL. Evolution of porous fractal properties during coal devolatilization. *Fuel*. 2008;87:878-84.

[13] Fu P, Hu S, Xiang J, Sun LS, Su S, Wang J. Evaluation of the porous structure development of chars from pyrolysis of rice straw: Effects of pyrolysis temperature and heating rate. *J Anal Appl Pyrolysis*. 2012;98:177-83.

[14] Fu P, Hu S, Xiang J, Yi WM, Bai XY, Sun LS, et al. Evolution of char structure during steam gasification of the chars produced from rapid pyrolysis of rice husk. *Bioresour Technol*. 2012;114:691-7.

[15] Yin YS, Zhang J, Sheng CD. Effect of pyrolysis temperature on the char micro-structure and reactivity of NO reduction. *Korean J Chem Eng*. 2009;26:895-901.

[16] Feng B, Bhatia SK, Barry JC. Variation of the crystalline structure of coal char during gasification. *Energy Fuels*. 2003;17:744-54.

[17] Wu SY, Gu J, Zhang X, Wu YQ, Gao JS. Variation of carbon crystalline structures and CO₂ gasification reactivity of Shenfu coal chars at elevated temperatures. *Energy Fuels*. 2008;22:199-206.

[18] Oya A, Mochizuki M, Otani S, Tomizuka I. Electron-microscopic study on the turbostratic carbon formed in

phenolic resin carbon by catalytic action of finely dispersed nickel. *Carbon*. 1979;17:71-6.

[19] Wang J, Morishita K, Takarada T. High-temperature interactions between coal char and mixtures of calcium oxide, quartz and kaolinite. *Energy Fuels*. 2001;15:1145-52.

[20] Sing KSW. Reporting physisorption data for gas solid systems - with special reference to the determination of surface-area and porosity. *Pure and Applied Chemistry*. 1982;54:2201-18.